

Experimental assisted design development for a 3D reticulate octahedral cellular structure using additive manufacturing

Li Yang

Department of Industrial Engineering, University of Louisville, Louisville, KY 40292

REVIEWED

Abstract

Traditionally it has been difficult to develop and verify designs for 3D reticulate cellular structure. Additive manufacturing provided a feasible alternative for this challenge. In this work, a 3D octahedral cellular structure was designed and investigated. Using a combined method of simulation and experimentation, the mechanical properties of the structures were evaluated. It was found that the cellular structure exhibits unusual size effect that is highly predictable by simulation and experimentation. This work established the design-property mapping for the octahedral cellular structure for further design development, and demonstrated the feasibility of applying this type of structure in sandwich panel applications.

Introduction

Cellular structures have been drawing increasing attentions in recent years due to their potentials in high performance-to-weight ratio applications. Sometimes referred to as “metamaterials”, cellular structures could achieve tailored physical and mechanical properties via the control of interior geometries [1, 2]. Additive manufacturing (AM) has been increasingly often used to manufacture cellular structures due to its freeform capability with complex geometries [3-6]. On the other hand, the design theory for cellular structures is relatively underdeveloped, especially for the cellular structures with 3D architectures. By far only several of such 3D cellular structures have been investigated in details for design development, including octet-truss structures [7-10] and re-entrant auxetic structures [4, 11-14]. It has been suggested that the development of design tools for 3D cellular structures could be facilitated by AM technologies [15]. With the fabrication capability of AM, cellular designs could be verified by experimentation, and other non-geometrical design factors such as manufacturing factors and boundary factors could be conveniently identified and investigated. In this paper, works were focused on the preliminary modeling of an octahedron 3D cellular structures with electron beam melting (EBM) process. The octahedral structure was of interest to this study due to its relatively straightforward deformation mechanism and the potentials in high energy absorption sandwich structure applications. The approach of this study took the same methodology used previously in the development of auxetic structure with EBM [4, 11-14], in which analytical modeling, finite element analysis and experimentation were used in combination in order to gain insights into the design issue.

Modeling of structure

The octahedral structure is a special type of 3D cellular structures. Unlike many other commonly seen cellular structures, this octahedral structure does not have tetrahedral or triangular sub-structures. As shown in Fig.1(b), the octahedral structure can be represented by an octahedral volume with eight sloped struts. This structure has been previously studied experimentally, although the work was focused on process perspectives [16] The Maxwell stability criterion number for the octahedral structure is $M < 0$ [17], which indicates that the structure does not have the same kinematic stability as compared to some of the other 3D cellular structures such as octet-truss. It's worth noting that for structural analysis purpose, the unit cell of the octahedral cellular structure could be constructed around a joint. As shown in Fig.1(c), the unit cell structure possesses a central joint with eight struts radiate out. From the construction of the unit cell, it is obvious that the octahedral structure has the same geometrical patterns in all the three principal directions, and therefore would exhibit the same loading response mechanism in all the three principal directions. As a result, for the purpose of modeling, only one principal direction needs to be investigated.

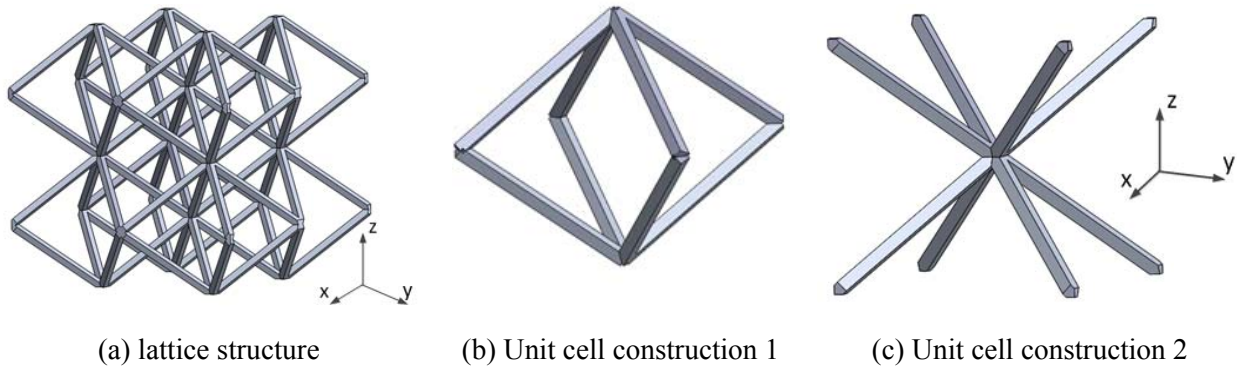


Fig.1 Octahedral cellular structure

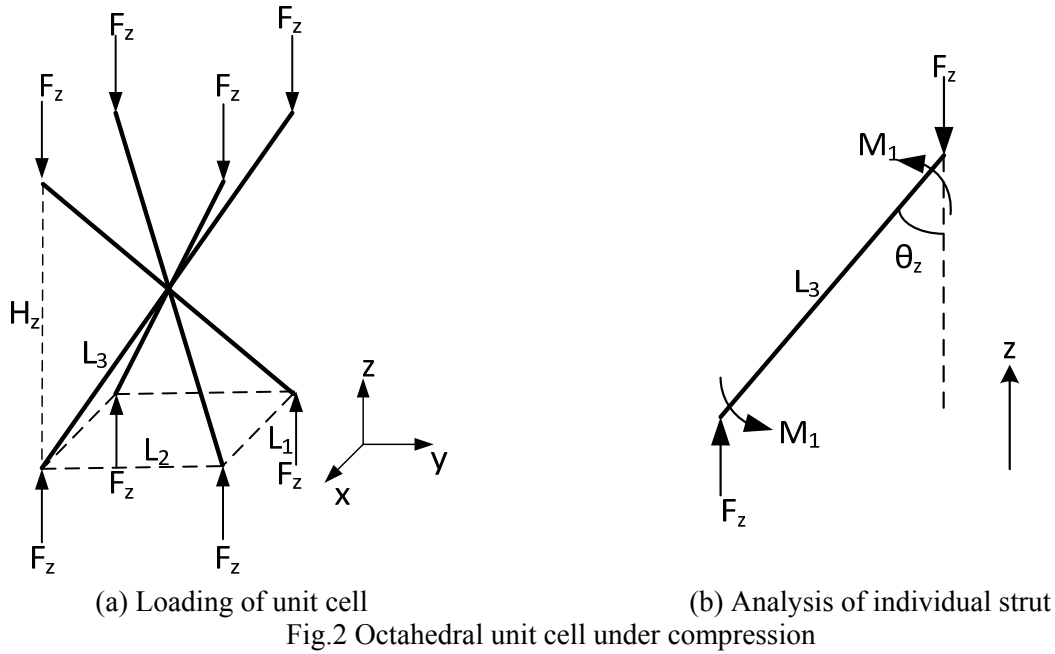
In this study, work was focused on the uniaxial properties of the structure. Consider a remote compressive stress σ applied on the structure along the z direction. The loading of the unit cell structure is shown in Fig.2(a). From structural symmetry, it is apparent that all the struts are under the same loading conditions. Fig.2(b) further illustrates the loading condition of an arbitrary strut. From Fig.2, the following force components could be obtained:

$$F_z = \frac{1}{4} \sigma_z L_1 L_2 \quad (1)$$

$$M_1 = \frac{1}{2} F_z L_3 \sin \theta_z = \frac{1}{8} \sigma_z L_1 L_2 L_3 \sin \theta_z \quad (2)$$

where L_1, L_2 , are the dimensions of the unit cell in x and y directions, and L_3 is the length of a half-strut, and θ_z is the slope angle of the strut in relation to the z axis:

$$\theta_z = \sin^{-1} \frac{\sqrt{L_1^2 + L_2^2}}{2L_3} \quad (3)$$



Under the loading condition shown in Fig.2(b), the strut undergoes a bending/shearing combined deformation. It has been shown before that the deformation along the strut axis is insignificant for metal cellular structures under non-catastrophic stress levels, therefore is not considered [18]. Apply Timoshenko beam analysis, the deformation of the strut in the z direction and the direction perpendicular to the z direction (not labeled in Fig.2(b)) can be obtained as:

$$\Delta z = L_3 \sin \theta_z \left(\frac{M_1 L_3}{6EI} + \frac{6F_z \sin \theta_z}{5GA} \right) \quad (3)$$

$$\Delta z_{\perp} = L_3 \cos \theta_z \left(\frac{M_1 L_3}{6EI} + \frac{6F_z \sin \theta_z}{5GA} \right) \quad (4)$$

where E , G are the modulus of elasticity and shear modulus of the solid material, I is the second moment of inertia of bending in the plane shown in Fig.2(b), and A is the cross sectional area. If the deflection Δz_{\perp} is further decomposed into deformations in the x and y directions, Δx and Δy , then:

$$\Delta x = L_3 \cos \beta_z \cos \theta_z \left(\frac{M_1 L_3}{6EI} + \frac{6F_z \sin \theta_z}{5GA} \right) \quad (5)$$

$$\Delta y = L_3 \sin \beta_z \cos \theta_z \left(\frac{M_1 L_3}{6EI} + \frac{6F_z \sin \theta_z}{5GA} \right) \quad (6)$$

Therefore, the modulus of the unit cell can be expressed as:

$$E_z = \frac{L_3 \cos \theta_z \sigma_z}{\Delta z} = \frac{H_z \sigma_z}{2\Delta z} = \frac{H_z}{2L_1 L_2 L_3 \sin^2 \theta \left(\frac{L_3^2}{48EI} + \frac{3}{10GA} \right)} \quad (7)$$

Where $H_z = 2L_3 \cos \theta = 2\sqrt{L_3^2 - \frac{1}{4}(L_1^2 + L_2^2)}$, as is also shown in Fig.2(a).

The strength of the structure could be roughly estimated as the onset of the yield in arbitrary strut. This could provide an estimation of yield strength of the structure. Since it is known that thin features produced by EBM process exhibit significant surface defects [18-21], it is reasonable to use more conservative estimations for the strength prediction of cellular structures. The normal and shear stress of the strut shown in Fig.2(b) can be determined from the bending moment, normal force and shear force as:

$$\sigma_1 = \frac{M_1 u}{I} + \frac{F_z \cos \theta_z}{A} = \frac{\sigma_z L_1 L_2 L_3 \sin \theta_z}{8I} u + \frac{\sigma_z L_1 L_2 \cos \theta_z}{4A} \quad (8)$$

$$\tau_1 = \frac{F_z \sin \theta_z D}{Ib} \quad (9)$$

Where u is the distance from the geometrical center of the cross section to the location of interest, D is the moment of area of the cross section, and b is the width of the cross section at the location of interest. Apply Von Mises Criterion, the maximum allowable stress level σ_m that results in the onset of structure yield is:

$$\sigma_m = \frac{4}{L_1 L_2 \sqrt{\frac{L_3^2 \sin^2 \theta_z}{2I^2} u^2 + \frac{2 \cos^2 \theta_z}{A^2} + \frac{6 \sin^2 \theta_z D^2}{I^2 b^2}}} \sigma_Y \quad (10)$$

Fig.3 and Fig.4 show the modulus and yield strength of the octahedral structures as functions of geometrical design parameters. The mappings were generated to illustrate the range of mechanical properties achievable by geometrical designs, and it is obvious from the modeling that the mechanical properties of the octahedral structures could be tailored at a wide range. The deformation of the octahedral structure is largely dominated by bending and shearing, therefore it is a bending dominated cellular structure [17]. The complete lack of tension-compression strut in the unit cell also determines that bending/shearing is the only active deformation mechanism for the octahedral cellular structure. It was predicted that bending dominated structures could dissipate considerable amount of energy upon plastic deformations, therefore, the octahedral structure might possess good potential in energy absorption applications.

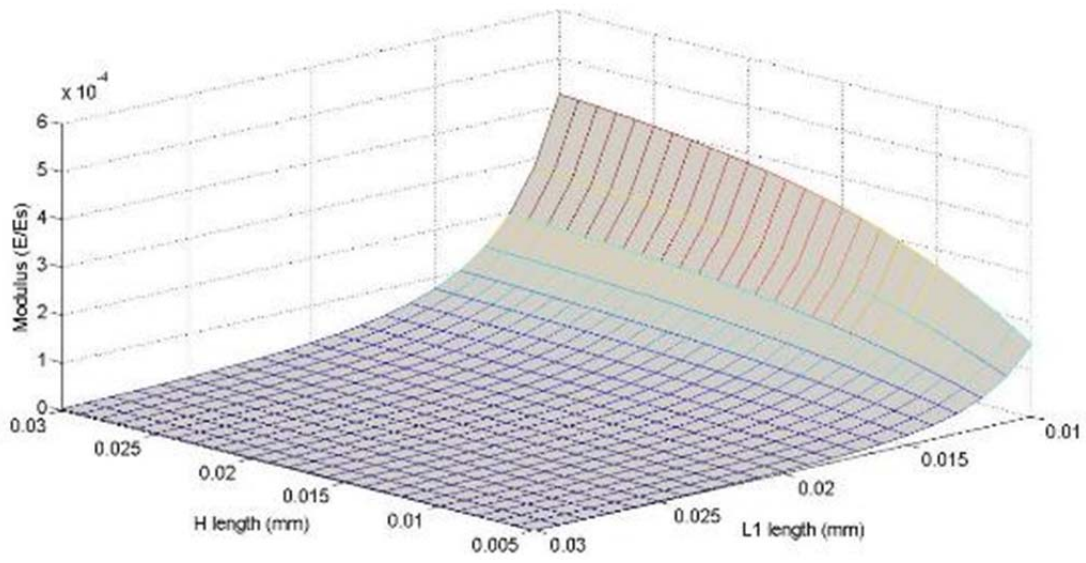


Fig.3 Modulus of the octahedral structure

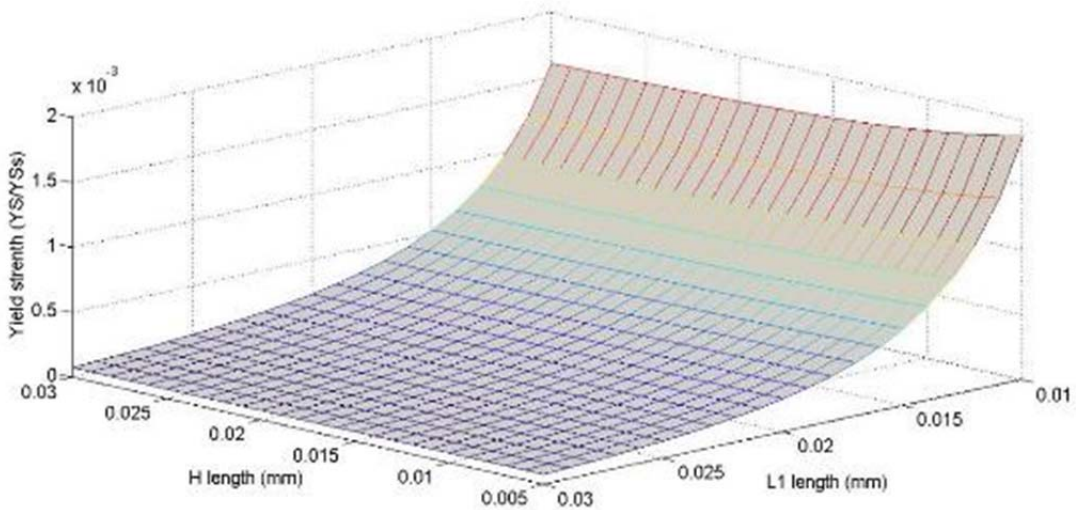


Fig.4 Yield strength of the octahedral structure

Another interesting characteristic of the octahedral structure also originates from its geometry. Throughout the modeling process, no assumption of infinite structure was required, which is often adopted for the other cellular structures in order to simplify the modeling. As a result, the equations derived for the octahedral structure is expected to be applicable for even lattices with small numbers of unit cell repetitions. This is in significant contrast with the general theory for cellular structures, in which about 8-10 unit cells are required in order for the structures to minimize the boundary effects [22, 23]. This property could also be very useful in applications, especially for the design of sandwich structures with very limited spaces. For these structures, only one or two layers of periodic cellular cores are often

allowed, and the ability to accurately predict the mechanical properties of the core structure at this scale is highly desired.

In order to verify this observation, finite element analysis (FEA) was performed with octahedral structures of various sizes. Models with unit cell numbers ($x \times y \times z$) of $1 \times 1 \times 1$, $2 \times 2 \times 1$, $4 \times 4 \times 1$, $8 \times 8 \times 1$, $1 \times 1 \times 2$, $2 \times 2 \times 2$, $4 \times 4 \times 2$, $8 \times 8 \times 2$, $1 \times 1 \times 4$, $2 \times 2 \times 4$, $4 \times 4 \times 4$, $8 \times 8 \times 4$ and $8 \times 8 \times 8$ were constructed and analyzed in SolidWorks using COMSOL simulation module. The numbers of unit cell repetition was chosen for the easiness of modeling. The simulations were performed with an office workstation, and it was noted that the computational load of the simulation quickly exceeded the practical level when the total number of unit cell exceeded the 512 level. Therefore, no simulations beyond $8 \times 8 \times 8$ were performed. An arbitrary unit cell design was used for the simulations with $L_1=20\text{mm}$, $L_2=18.74\text{mm}$, $H=20\text{mm}$ and square strut of $t=1\text{mm}$. While the type of material is not of concern of the simulation, the material was defined as Al-6061-T6 alloy. In the simulation, a curvature based mesh with mesh size of 0.9mm was used throughout the simulation. The mesh size was tested by performing static compression simulations with different mesh sizes, and it was found that the results of the relatively coarse 0.9mm mesh size were adequately accurate for the purpose of this study. Fig.5 shows the boundary condition setup for the simulation. The structure was bonded to the two platens on both sides of the loading direction, and the stiffness of the platens was set to be significantly higher than the structure material in order to minimize the analysis error. One platen was fixed, and the other was loaded with uniaxial compressive stress. Since elastic analysis was performed, only the size effect of elastic modulus was verified.

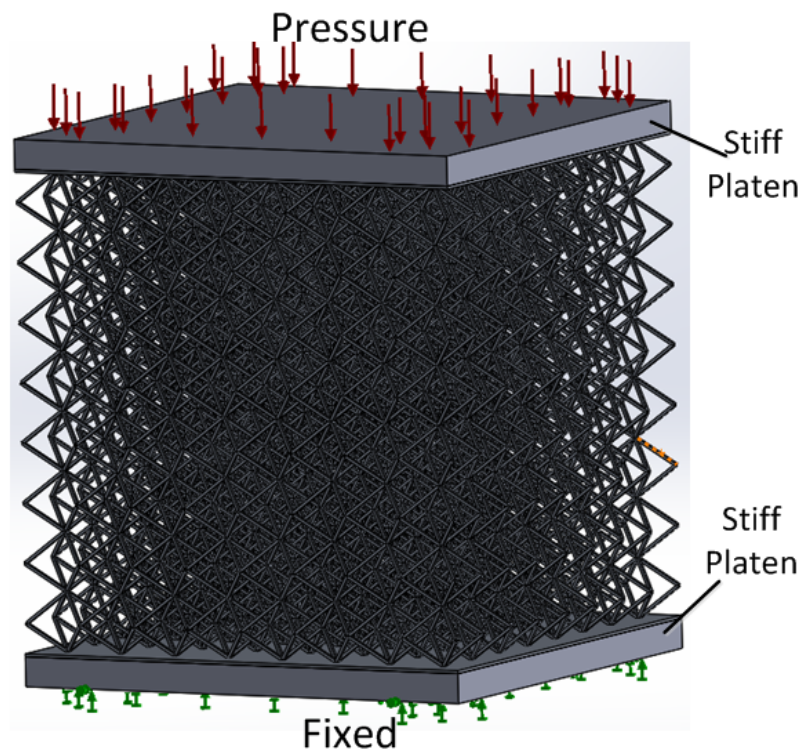
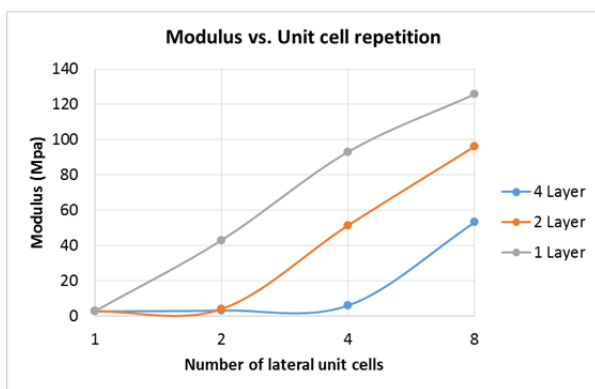


Fig.5 Boundary condition setup for the FEA simulation of size effect

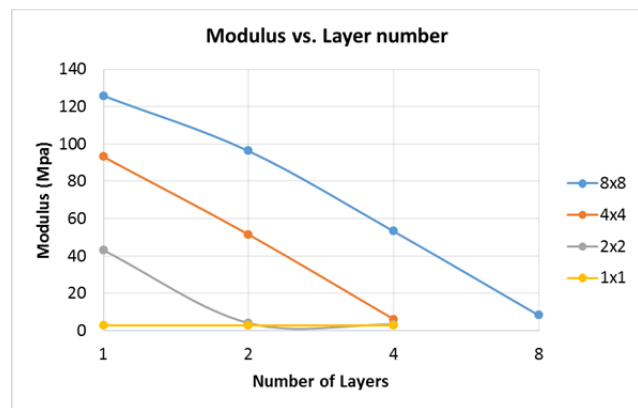
The results of the simulation are listed in Table 1. It was found that despite the prediction, the octahedral structure exhibits significant size effect. However, upon close look, the octahedral structures exhibit a counterintuitive size effect in the direction of the loading. While the modulus of the structure increases with increased number of unit cells parallel to the loading direction, it exhibits a steady reducing trend as the number of unit cells in the loading direction (z direction) increases, which is further illustrated in Fig. 6. For regular cellular structures, size effect tends to soften the structure due to the loss of symmetry at the boundaries. However, for octahedral structure, there exists an opposite trend. With fewer numbers of layers, the structure actually becomes stiffer. It was also observed that the size effects in both cases follow a very predictable logarithm trend. This unconventional phenomenon was mentioned in previous studies with similar structures, although no further details were discussed [25].

Design	FEA modulus (MPa)	Calculated modulus (MPa)	FEA modulus – Free boundary (MPa)
1x1x1	2.751	2.300	2.563
1x1x2	2.721	2.300	2.623
1x1x4	2.702	2.300	2.654
2x2x1	42.955	2.300	2.620
2x2x2	3.992	2.300	2.685
2x2x4	3.256	2.300	2.714
4x4x1	93.067	2.300	2.656
4x4x2	51.394	2.300	2.719
4x4x4	6.024	2.300	2.742
8x8x1	125.786	2.300	-
8x8x2	96.177	2.300	-
8x8x4	53.121	2.300	-
8x8x8	8.060	2.300	-

Table 1 Size effect evaluation for octahedral structure



(a) Lateral size effect



(b) Layer-wise size effect

Fig.6 Size effect of the octahedral structure modulus by FEA

Further investigation revealed the cause of this unconventional size effect. As shown in Fig.7, when the number of layers increases, the octahedral structure starts to exhibit specific diagonal pattern of stress

concentration. On the other hand, when the boundary conditions were adjusted to allow for relative sliding between the compressive platens and the octahedral structures, this size effect largely disappeared, as shown in the last column of Table 1. This phenomenon is likely originated from the boundary restrictions. As is commonly known, a solid exhibits upsetting when compressed between two platens, which is caused by the friction between the solid and the platens [24]. The upsetting phenomenon does not appear to be reported in any previous studies, and it could be intriguing consider the fact that cellular structures are largely dis-continuous solids in 3D space, therefore the stress distribution would be largely geometry dependent. It was expected that this boundary effect would be difficult to eliminate in practice since for most applications the cellular structures would be restricted at the boundaries. However, due to the difficulty of modeling upsetting phenomenon, further works exceeded the scope of this paper, and will be addressed in future studies. On the other hand, the good predictability of this size effect as shown in Fig.6 suggested that a relatively effective design method could be developed based on a reasonable set of experiments.

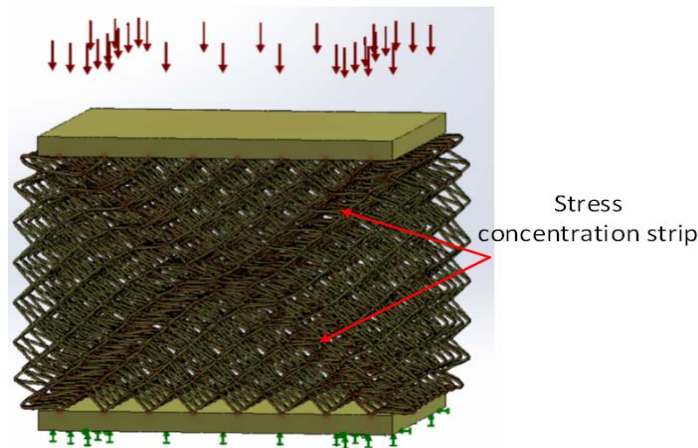


Fig.7 Stress concentration of octahedral structure

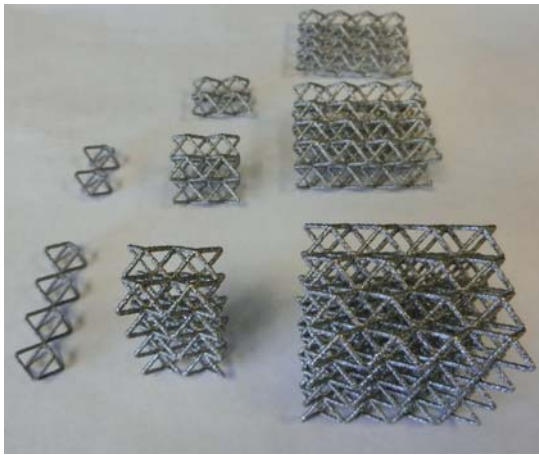
Experiments and discussions

A random parameter set was chosen to verify the accuracy of the modeling for the octahedral structure. The parameters and the theoretical predictions are shown in Table 2. The structures were modeled in SolidWorks and fabricated in the Arcam EBM S400 machine using Ti6Al4V-ELI as material. In the CAD models, the cross sections of the struts were designed to be square. However, due to the feature resolution limit of the EBM process, the actual strut cross sections of the samples exhibit irregular shapes, therefore a round cross section approximation was adopted in the calculation of models. Octahedral structures with 1x1x1, 1x1x2, 1x1x4, 2x2x1, 2x2x2, 2x2x4, 4x4x1, 4x4x2, 4x4x4 numbers of unit cells were designed, and the samples were fabricated in three builds, with one sample for every design fabricated in each build.

Design	L_1 (mm)	L_2 (mm)	H (mm)	t (mm)	Theo. Modulus (MPa)	Theo. Strength (MPa)
	10	8	10	1	44.773	1.935

Table 2 Design parameters for the octahedral samples

Fig.8(a) shows the fabricated octahedral lattice samples. The overall dimensions of each fabricated sample were measured by caliper. Compressive test was performed for the samples with an Instron 5569A universal tester. The samples were fixed between two steel platens, 50000N load cell was used for samples with 4 unit cell lateral repetitions, and 5000N load cell was used for the other samples. The displacement of the crosshead was used as the total deformation of the structures consider the small modulus of tested samples. Fig.8(b) shows the actual setup of the compressive testing for the octahedral lattices. The testing results are shown in Table 3. The dimensions and mechanical properties of the samples were quite consistent, indicating a relatively stable manufacturing quality at strut size of 1mm. It was assumed that the mechanical properties of the Ti6Al4V material fabricated by EBM is isotropic, therefore the results obtained from experimentation could be directly compared with the prediction.



(a) Octahedral lattice



(b) Compressive test

Fig.8 Octahedral lattices for experimental verification

Design	$D1$ (mm)	$D2$ (mm)	$D3$ (mm)	Modulus (MPa)	Strength (MPa)
1x1x1	7.86±0.01	9.94±0.04	9.68±0.06	27.27±0.34	1.53±0.01
1x1x2	7.90±0.07	9.92±0.04	19.88±0.18	28.76±0.55	1.63±0.08
1x1x4	7.92±0.05	9.90±0.06	40.08±0.20	31.41±1.14	1.11±0.11
2x2x1	19.82±0.01	15.80±0.03	9.72±0.16	33.46±1.82	2.24±0.05
2x2x2	19.80±0.03	15.79±0.02	19.73±0.11	34.61±1.69	1.93±0.04
2x2x4	19.94±0.06	15.75±0.03	40.18±0.19	37.96±0.78	2.00±0.01
4x4x1	31.67±0.05	39.58±0.06	9.89±0.21	39.42±3.79	3.10±0.37
4x4x2	31.60±0.03	39.54±0.05	19.83±0.13	37.41±1.50	2.32±0.03
4x4x4	31.66±0.03	39.61±0.07	40.18±0.18	39.11±1.16	2.39±0.08

Table 3 Compressive testing results for octahedral lattice

Due to the difficulty of sample orientation with the large aspect ratio designs (1x1x2 and 1x1x4) during compressive testing, the results for these samples were expected to have relatively large errors. In

addition, it was also observed that the samples of 1x1x4 design exhibited macroscopic elastic buckling during the compression test, which explained the considerably lower strength of the 1x1x4 design compared to the other designs. Overall, the modulus and strength values of the samples are close to the theoretical predictions, and no significant size effect was observed. Upon close inspection, it was found that the compressive test platens were indented and scratched during the compressive testing, which indicated that under the combination of shearing and compressive stress, there existed relative motions between the samples and the platen surfaces. Therefore, although the octahedral lattice samples still exhibited stress concentration patterns as shown in Fig.9, the boundary constraints were not ideal due to the relative motion between the samples and the platens, which resulted in mechanical properties that are somewhat close to the theoretical prediction.

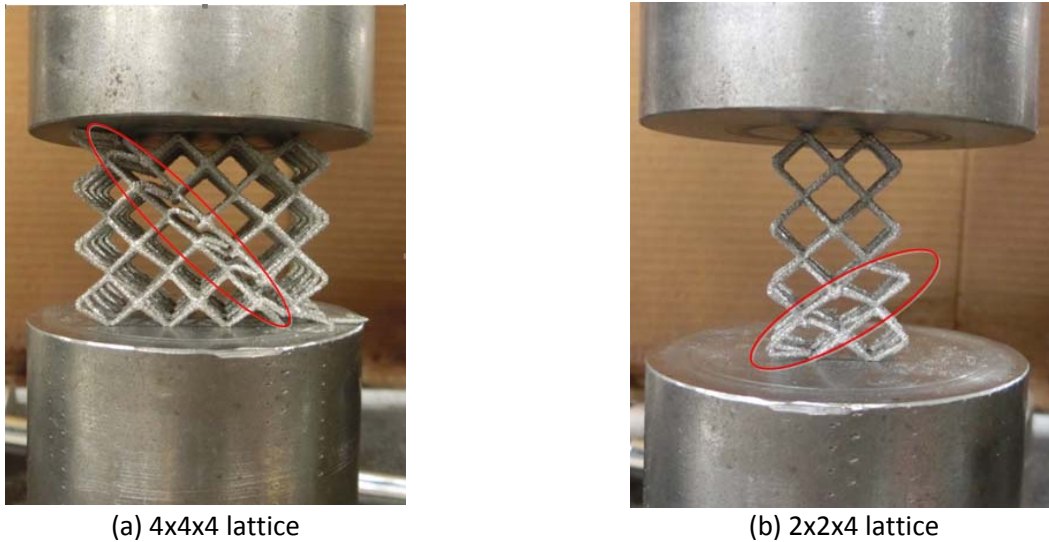
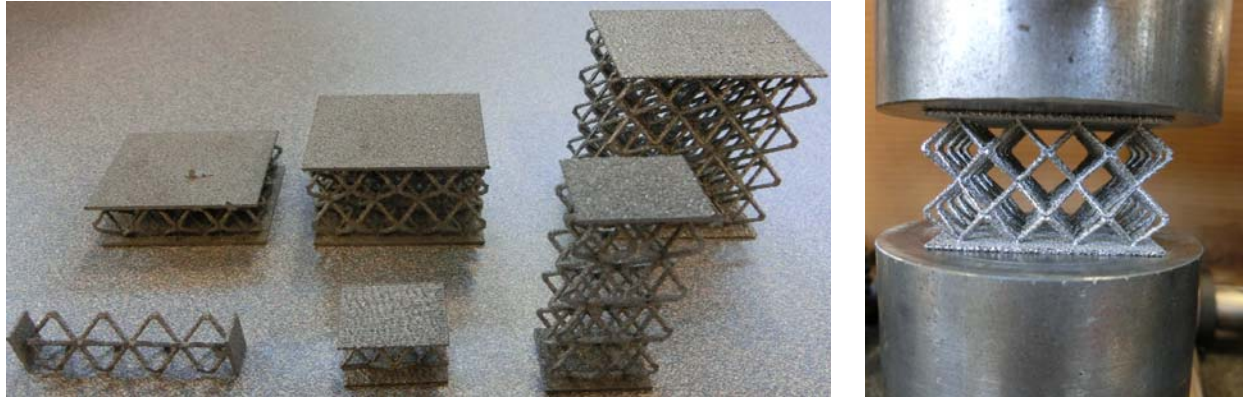


Fig.9 Stress concentration pattern of octahedral lattice during compression

Consider the fact that in actual applications the octahedral structures are likely to be fully constrained, the relative motions between the cellular structures and the surrounding structures will not be acceptable. Therefore, a second set of experiments were performed with redesigned samples. In order to ensure full constraint of the octahedral lattices, sandwich panel structures were designed. For the core of the sandwich structures, the same octahedral designs were adopted. The skin thickness of the sandwich structures were 1mm for all the designs. The designs were fabricated with the same process parameters and build setups. Since the skins were also thin features, all the samples were fabricated using the default network process theme provided by the machine. The sandwich models were rotated so that the skins aligned in the vertical orientations, therefore eliminated the potential issue with support requirements. The fabricated samples were measured and tested in the same manner. Fig.10 shows the fabricated sandwich samples and the setup for the compressive test.

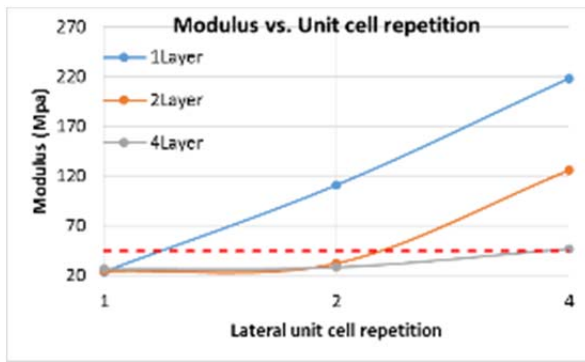


(a) Fabricated sandwich samples (b) Compressive test
 Fig.10 Octahedral sandwiches for experimental verification

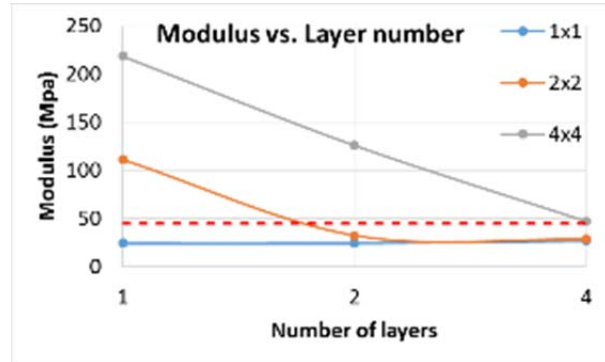
The results of the experiment are listed in Table 4. As could be observed clearly, the octahedral sandwich structures exhibited significant size effect. Fig.11 further illustrates the size effects of elastic modulus for the octahedral sandwiches. The size effect clearly showed the same pattern and logarithm trend as indicated by the predictions (Fig.6), and it was obvious that the size effect becomes apparent when the total number of layers exceeds the lateral unit cell repetition. In fact, from Table 4 it was also apparent that the strength of the octahedral sandwich also exhibits the same size effect, which is plotted in Fig.12 for clarity of information. With more unit cell repetitions in the lateral directions or less layers, the octahedral sandwich becomes stronger in compression. It could also be observed from Fig.11 that when the size effect of the octahedral sandwich is minimized, the modulus values of the sandwich structures are consistently lower than the predicted value (44.773MPa). This could be partly contributed by the manufacturing defects. It has been reported that cellular structures fabricated by EBM process possess a variety of defects [11, 13, 15, 18], which could significantly affect the mechanical properties of the parts. In addition, due to the build orientations selected, one side of the octahedral core of each sample was in contact with the substrate. Upon the parts removal, the joints of the octahedral lattices on these sides were partly damaged. For samples with large lateral unit cell repetitions, the effect of such defects was reduced. However, with smaller samples, these defects were more likely to result in the loss of mechanical performance, as was clearly suggested in the experimental results.

Design	$D1$ (mm)	$D2$ (mm)	$D3$ (mm)	Modulus (MPa)	Strength (MPa)
1x1x1	7.11 ± 0.13	9.88 ± 0.00	12.11 ± 0.02	24.23 ± 1.63	1.39 ± 0.17
1x1x2	7.25 ± 0.21	9.94 ± 0.14	22.29 ± 0.10	24.35 ± 2.40	1.35 ± 0.02
1x1x4	7.30 ± 0.23	9.97 ± 0.20	42.44 ± 0.43	26.74 ± 3.78	1.42 ± 0.13
2x2x1	15.56 ± 0.83	19.86 ± 0.04	12.32 ± 0.02	111.23 ± 2.02	3.79 ± 0.16
2x2x2	15.30 ± 0.29	19.85 ± 0.04	22.38 ± 0.03	32.49 ± 1.18	1.59 ± 0.06
2x2x4	15.31 ± 0.37	19.89 ± 0.03	42.79 ± 0.06	28.45 ± 1.16	1.57 ± 0.07
4x4x1	30.88 ± 0.22	39.63 ± 0.12	12.15 ± 0.01	132.28 ± 8.39	
4x4x2	31.15 ± 0.28	39.69 ± 0.03	22.38 ± 0.04	125.98 ± 1.18	3.60 ± 0.21
4x4x4	31.09 ± 0.33	39.63 ± 0.06	42.73 ± 0.01	47.15 ± 1.29	2.72 ± 0.12

Table 4 Table 3 Compressive testing results for octahedral sandwich

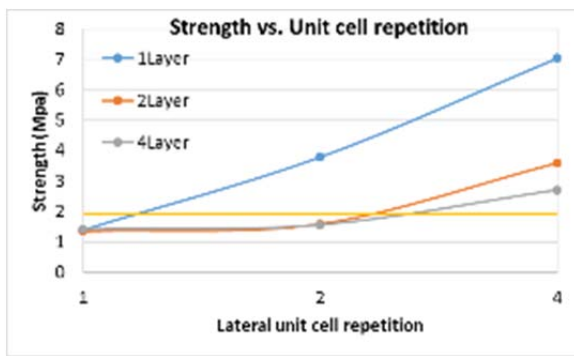


(a) Lateral size effect

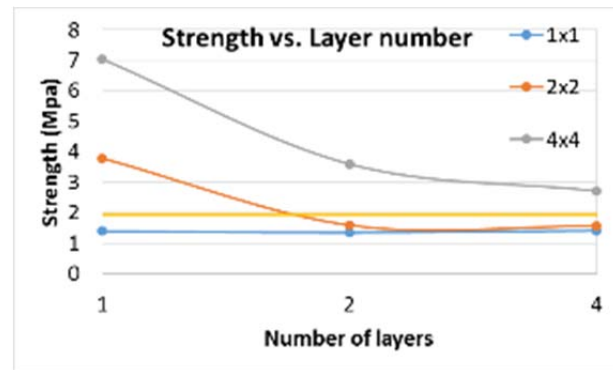


(b) Layer-wise size effect

Fig.11 Size effect of the octahedral sandwich modulus by experimentation



(a) Lateral size effect



(b) Layer-wise size effect

Fig.12 Size effect of the octahedral sandwich strength by experimentation

Conclusions

The design of cellular structures with AM technologies possesses great potential for many future applications with high performance lightweight structures. In this study, an octahedral cellular structure was modeled and tested. Using a combination of theoretical modeling, simulation and experimentation, insights were efficiently obtained for this cellular structure. Modeling work successfully established an accurate analytical model for the modulus prediction of the octahedral structure. It was also found that the octahedral cellular structure exhibits a highly predictable size effect, which could be utilized in the design of sandwich structures with thickness restrictions. The good agreement between the experiment and the theory for the octahedral structure also enables high fidelity design and manufacturing of this type of cellular structures for applications.

Acknowledgement

This study was performed in the Rapid Prototyping Center (RPC) in University of Louisville, and the author would like to acknowledge Tim Gornet, Joe Vicars, Gary Graf of the RPC and Hengfeng Gu for their support and help with this project.

Reference

- [1] Lorna J. Gibson. Cellular solids: structure and properties, 2nd edition. Cambridge University Press, New York, NJ, USA. 1997.
- [2] M.F. Ashby, A. G. Evans, N. A. Fleck, L. J. Gibson, J. W. Hutchinson, H. N. G. Wadley. Metal Foams: A Design Guide. Butterworth-Heinemann, Boston, US. 2000.
- [3] O. Cansizoglu, O. Harrysson, D. Cormier, H. West, T. Mahale. Properties of Ti-6Al-4V non-stochastic lattice structures fabricated via electron beam melting. *Materials Science and Engineering: A*, 492(2008), 1-2: 468-474.
- [4] L. Yang, D. Cormier, H. West, K. Knowlson. Non-stochastic Ti6Al4V foam structure that shows negative Poisson's Ratios. *Materials Science and Engineering: A*, 558(2012): 579-585.
- [5] Jens Bauer, Stefan Hengsbach, Iwiza Tesari, Ruth Schwaiger, Oliver Kraft. High-strength cellular ceramic composites with 3D microarchitecture. *Proceedings of the National Academy of Sciences of the United States of America*. 111(2014), 7: 2453-2458.
- [6] 3D printed nanostructured materials.
<http://www.engineering.com/3DPrinting/3DPrintingArticles/ArticleID/7832/3D-Printed-Nanostructured-Materials-Are-Strong-Light-Have-Many-Uses.aspx>.
- [7] V. S. Deshpande, N. A. Fleck, M. F. Ashby. Effective properties of the octet-truss lattice material. *Journal of the Mechanics and Physics of Solids*. 49(2001): 1747-1769.
- [8] V. S. Dashpande, N. A. Fleck. Collapse of truss core sandwich beams in 3-point bending. *International Journal of Solids and Structures*. 38(2001): 6275-6305.
- [9] R. G. Hutchinson, N. A. Fleck. The structural performance of the periodic truss. *Journal of the Mechanics and Physics of Solids*. 54(2006): 756-782.
- [10] H. V. Wang, C. Williams, D. W. Rosen. Design synthesis of adaptive mesoscopic cellular structures with unit truss approach and particle swarm optimization. *Proceedings of the 17th International Solid Freeform Fabrication (SFF) Symposium*. Austin, Texas, USA, 2006.
- [11] L. Yang, O. Harrysson, H. West II, D. Cormier. Design and characterization of orthotropic re-entrant auxetic structures made via EBM using Ti6Al4V and pure copper. *Proceedings of the 22nd International Solid Freeform Fabrication (SFF) Symposium*. Austin, Texas, USA, 2011.
- [12] L. Yang, O. Harrysson, H. West, D. Cormier. Modeling of uniaxial compression in a 3D periodic re-entrant lattice structure. *Journal of Materials Science*. 48(2013): 1413-1422.
- [13] L. Yang, O. Harrysson, D. Cormier, H. West. Compressive properties of Ti6Al4 auxetic mesh structures made by EBM process, *Acta Materialia*, 60(2012), 8: 3370-3379.
- [14] L. Yang, O. Harrysson, H. West, D. Cormier. A comparison of bending properties for cellular core sandwich panels. *Materials Science and Applications*. 4(2013), 8: 471-477.

- [15] Li Yang. Lightweight cellular structures with additive manufacturing: New design freedoms. RAPID Conference and Exposition. Detroit, USA, 2014.
- [16] S. Tsopanos, R. A. W. Mines, S. McKown, Y. Shen, W. J. Cantwell, W. Brooks, C. J. Sutcliffe. The influence of processing parameters on the mechanical properties of selectively laser melted stainless steel microlattice structures. *Journal of Manufacturing Science and Engineering*. 132(2010): 041011-1.
- [17] M. F. Ashby. The properties of foams and lattices. *Philosophical Transactions of The Royal Society A*. 364(2006): 15-30.
- [18] Li Yang. Design, Structural Design, Optimization and Application of 3D Re-entrant Auxetic Structures. PhD Dissertation, North Carolina State University. Raleigh, NC, USA, 2011.
- [19] Denis Cormier, Harvey West, Ola Harrysson, Kyle Knowlson. Characterization of thin walled Ti-6Al-4V components produced via electron beam melting. *Proceedings of the 15th International Solid Freeform Fabrication (SFF) Symposium*. Austin, Texas, USA, 2004.
- [20] O. Cansizoglu, D. Cormier, O. Harrysson, H. West, T. Mahale. An evaluation of non-stochastic lattice structures fabricated via electron beam melting. *Proceedings of the 17th International Solid Freeform Fabrication (SFF) Symposium*. Austin, Texas, USA, 2006.
- [21] S. J. Li, L. E. Murr, X. Y. Cheng, Z. B. Zhang, Y. L. Hao, R. Yang, F. Medina, R. B. Wicker. Compression fatigue behavior of Ti-6Al-4V mesh arrays fabricated by electron beam melting. *Acta Materialia*. 60(2012): 793-802.
- [22] Gaoming Dai, Weihong Zhang. Size effects of effective Young's modulus for periodic cellular structures. *Science in China Series G: Physics, Mechanics & Astronomy*. 52(2009), 8: 1262-1270.
- [23] P. R. Onck, E. W. Andrews, L. J. Gibson. Size effects in ductile cellular solids. Part I: modeling. *International Journal of Mechanical Sciences*. 43(2001): 681-699.
- [24] Jerzy Kajtoch. Strain in the upsetting process. *Metallurgy and Foundry Engineering*. 33(2007), 1: 51-61.
- [25] S. Tsopanos, R. A. W. Mines, S. McKown, Y. Shen, W. J. Cantwell, W. Brooks, C. J. Sutcliffe. The influence of processing parameters on the mechanical properties of selectively laser melted stainless steel microlattice structures. *Journal of Manufacturing Science and Engineering*. 132(2010): 041011.